Available online at www.sciencedirect.com
ScienceDirect
Bioorganic & Medicinal Chemistry Letters 18 (2008) 3206–3210
Bioorganic & Medicinal Chemistry Letters

Verification of the C-terminal intramolecular β-sheet in Aβ42 aggregates using solid-state NMR: Implications for potent neurotoxicity through the formation of radicals

Yuichi Masuda,[a] Satoko Uemura,[a] Azusa Nakanishi,[b] Ryutaro Ohashi,[b] K. Takegoshi,[b] Takahiko Shimizu,[c,d] Takuji Shirasawa[c,e] and Kazuhiro Irie[a,*]

[a]*Division of Food Science and Biotechnology, Graduate School of Agriculture, Kyoto University, Kyoto 606-8502, Japan*
[b]*Department of Chemistry, Graduate School of Science, Kyoto University, Kyoto 606-8502, Japan*
[c]*Research Team for Molecular Biomarkers, Tokyo Metropolitan Institute of Gerontology, Tokyo 173-0015, Japan*
[d]*Applied Biological Chemistry, United Graduate School of Agricultural Science, Tokyo University of Agriculture and Technology, Tokyo 183-8509, Japan*
[e]*Department of Ageing Control Medicine, Juntendo University Graduate School of Medicine, Tokyo 113-8421, Japan*

Received 22 March 2008; revised 19 April 2008; accepted 23 April 2008
Available online 26 April 2008

Abstract—Structural analysis of 42-residue amyloid β (Aβ42) aggregates using rotational resonance in solid-state NMR verified that C_β and/or C_γ of Met-35 and the carboxyl carbon of Ala-42 are proximal enough to form an intramolecular antiparallel β-sheet in the C-terminus. The *S*-oxidized radical cation at Met-35, an ultimate radical species responsible for neurotoxicity, could be stabilized by the carboxylate anion at the C-terminus, resulting in aggregation to cause long-term oxidative stress.

Alzheimer's disease (AD) is characterized by the abnormal deposition of 40- and 42-mer amyloid β peptides (Aβ40 and Aβ42) in the brain.[1] Since Aβ42 is far more aggregative and neurotoxic than Aβ40,[2] Aβ42 plays a critical role in the etiology of AD. Elucidation of the tertiary structure of Aβ42 aggregates is therefore a pressing need for understanding the mechanism of neurotoxicity and development of new therapeutic agents for AD. Numerous biophysical studies revealed that Aβ forms intermolecular β-sheets to aggregate.[3–5] Our systematic replacement of Aβ42 with proline proposed a model of Aβ42 aggregates related to neurotoxicity (Fig. 1A).[6] However, it remains unclear whether the C-terminal β-sheets at positions 35–37 and 40–42 are intramolecular or intermolecular.

Oxidative stress induced by Aβ has been implicated as a major cause of neurotoxicity in AD,[7,8] and a number of studies suggest the importance of Met-35. The sulfur atom of Met-35 is oxidized in the presence of metal ions to give the *S*-oxidized radical cation, which causes lipid peroxidation, protein oxidation, and free radical formation. However, this radical cation is too short-lived to cause toxic effects in neuronal cells, where diffusion is the rate-determining step for neurotoxicity because of the highly viscous environment.[9] Previous investigations suggested that *S*-oxidized radical cation could be stabilized by amide carbonyl oxygen or carboxylate anion by forming an S–O bond.[9–11]

In our model of Aβ42 aggregates (Fig. 1A), a turn structure exists between the two β-strands at positions 35–37 and 40–42.[6] This led us to suggest the formation of an intramolecular antiparallel β-sheet at positions 35–42 to enable the association of the sulfur atom of Met-35 with the C-terminal carboxylate anion, thereby stabilizing the radical cation by forming an S–O bond (Fig. 1B).[12] To verify this model, we examined the spatial proximity between the side chain of Met-35 and the carboxyl group of Ala-42 in Aβ42 aggregates using solid-state NMR.

Aβ42 peptides uniformly labeled with ^{13}C and ^{15}N at Met-35 and Ala-42 were prepared by solid-phase Fmoc synthesis as reported previously.[6] Since verification of

Keywords: Aβ42; Alzheimer's disease; Amyloid; β-Sheet; Rotational resonance; Solid-state NMR.
* Corresponding author. Tel.: +81 75 753 6281; fax: +81 75 753 6284; e-mail: irie@kais.kyoto-u.ac.jp

0960-894X/$ - see front matter © 2008 Elsevier Ltd. All rights reserved.
doi:10.1016/j.bmcl.2008.04.060

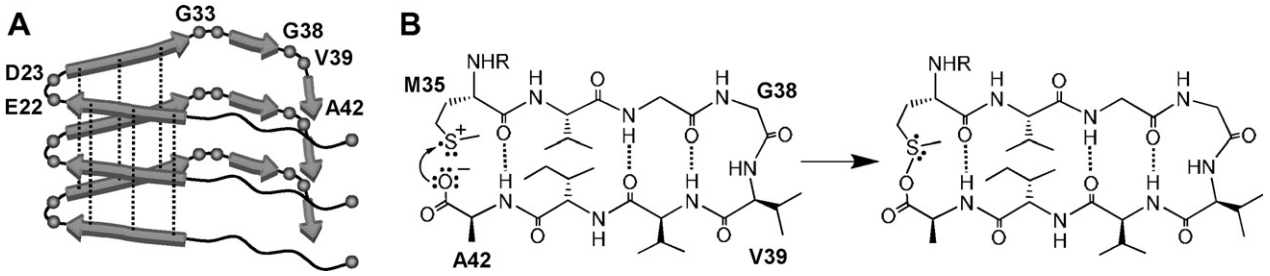

Figure 1. (A) The model of Aβ42 aggregates based on the systematic replacement with proline.[6] (B) Possible mechanism for stabilization of the radical species of Aβ42. The *S*-oxidized radical cation at Met-35 generated by redox reactions[7,8] is stabilized by the C-terminal carboxylate anion to form a hydrophobic core, resulting in long-term oxidative stress.[12] Dotted lines show hydrogen bonds in β-sheets.

the formation of the C-terminal intramolecular β-sheet in Aβ42 is the main purpose of this study, we used the sample, in which Met-35 and Ala-42 were uniformly labeled with ^{13}C and ^{15}N, in order to estimate roughly the vicinity of these residues. We labeled nitrogen atoms with ^{15}N to avoid the influence of the ^{14}N quadrupole interaction on ^{13}C.[13,14] Labeled Aβ42 (25 μM) aggregated completely at 37 °C in phosphate-buffered saline (pH 7.4) for 48 h. To eliminate intermolecular correlations, aggregates of labeled Aβ42 diluted with unlabeled Aβ42 at a ratio of 1:2 was also prepared. Typical formation of fibrils was confirmed by transmission electron microscopy (Fig. S1). After centrifugation followed by washing with distilled water, aggregates were dried in vacuo and subjected to solid-state NMR measurement.

^{13}C–^{1}H Dipolar assisted rotational resonance (DARR),[15] which realizes a broadband ^{13}C–^{13}C correlation, was used to assign the ^{13}C chemical shifts in the Aβ42 aggregates. All ^{13}C chemical shifts were assigned unambiguously from the 2D DARR experiments (Fig. S2 and Table 1). Two sets of chemical shifts were observed for Met-35; this indicates that Met-35 exists as two conformations or molecular species. Deviations of ^{13}C chemical shifts in peptides relative to those of their corresponding random coil ($\Delta\delta = \delta_{observed} - \delta_{random\ coil}$) correlate with the secondary structure. Wishart et al.[16,17] reported that $\Delta\delta$ of C_α and carbonyl carbons are positive in α-helices and negative in β-sheets, and that $\Delta\delta$ of C_β is negative in α-helices and positive in β-sheets. $\Delta\delta$ of $^{13}C_\alpha$ (−1.5, −2.5) and C=O (−3.5) at Met-35 were negative and $^{13}C_\beta$ at Met-35 (+3.4) was positive; this suggest that Met-35 could form β-sheet. Although the secondary structure at the C-terminal end is not precisely predictable from the chemical shifts, the negative $\Delta\delta$ of $^{13}C_\alpha$ (−0.5) and positive $\Delta\delta$ of $^{13}C_\beta$ (+1.7) at Ala-42 suggests that this residue could be included in β-sheet.

We adopted rotational resonance (R2) method to estimate the distance between the side chain of Met-35 and the carboxyl group of Ala-42 (Fig. 2).[18] In this experiment, the magic angle spinning (MAS) speed was set to the difference between the chemical shifts of the two ^{13}C spins of interest. Under the R2 condition, the magnetization transfer within the ^{13}C spins is driven selectively by the reintroduction of the dipole–dipole interaction. The difference in chemical shifts between ^{13}C pairs of interest should be larger than 10 kHz (100 ppm at 100 MHz for ^{13}C NMR) to minimize the spinning sidebands. In previous R2 experiments, magne-

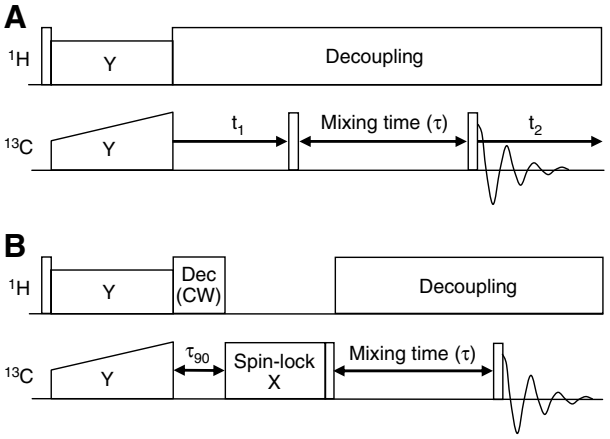

Figure 2. Pulse sequence for (A) 2D and (B) 1D R2 experiments.

Table 1. ^{13}C Chemical shifts [δ (ppm)] of Aβ42 aggregates[a]

Residue	C=O	C_α	C_β	C_γ	C_ε
Met-35 (conformer 1)[b]	171.2	52.3	34.7	30.4	16.9
Met-35 (conformer 2)	ND[c]	51.3	ND	32.2	17.6
	(174.7)[d]	(53.8)	(31.3)	(30.4)	(15.3)
Ala-42	179.5	50.4	19.2		
	(176.2)	(50.9)	(17.5)		

[a] TMS was used as an external standard.
[b] The ratio of the conformers was not determined, but the intensity of conformer 1 was slightly larger than that of conformer 2.
[c] The ^{13}C chemical shift could not be assigned because of weak signal intensity and/or signal broadening.
[d] Values in parentheses are chemical shifts in random-coil,[17] adjusted to the TMS reference.

tization transfers between spatially remote carbons up to 6 Å apart were normally detected.[19–21]

In our model of Aβ42 aggregates (Fig. 1B), the carbons in the side chain of Met-35 (C_β, C_γ, and C_ε) are close to C=O of Ala-42. If we applied the R2 experiment to C_ε of Met-35 and C=O of Ala-42, magnetization transfer between C_β and C=O of Ala-42 would also occur because of the similar chemical shifts of C_ε of Met-35 (δ 16.9, 17.6) and C_β of Ala-42 (δ 19.2). We therefore applied the R2 experiments to C_β and/or C_γ of Met-35 (δ 32.2: the center of the peaks) and C=O of Ala-42 (δ 179.5).

First, we carried out a 2D R2 experiment (Fig. 2A) at the mixing time of 50 ms under the R2 condition of C_β and/or C_γ of Met-35 and C=O of Ala-42 (Fig. 3A). A cross peak possibly caused by the R2 effect was observed (Fig. 3B, arrow). To verify whether this peak arises from noise or not, 1D R2 experiments at a variety of mixing times were performed (Fig. 4B–D). In order to detect magnetization transfer with high sensitivity, we maintained one of the ^{13}C magnetization using a spin-lock pulse until the other magnetization of interest had disappeared (Fig. 2B). Magnetization transfer was observed from C_β and/or C_γ of Met-35 to C=O of Ala-42, and the signal intensity became larger in proportion to increased mixing time (Fig. 4B–D). Reverse magnetization transfer from C=O of Ala-42 to C_β and/or C_γ of Met-35 was also observed (Fig. S3). These data strongly suggest that the cross peak in the 2D R2 experiment (Fig. 3A and B) arose from the dipole–dipole interaction. Moreover, we confirmed that magnetization transfer also occurred in the 1D R2 experiment using aggregates of labeled Aβ42 diluted with unlabeled Aβ42 at a ratio of 1:2 (Fig. 4E); this indicates that the dipole–dipole interaction detected in Figure 3 can be attributed to intramolecular carbons.

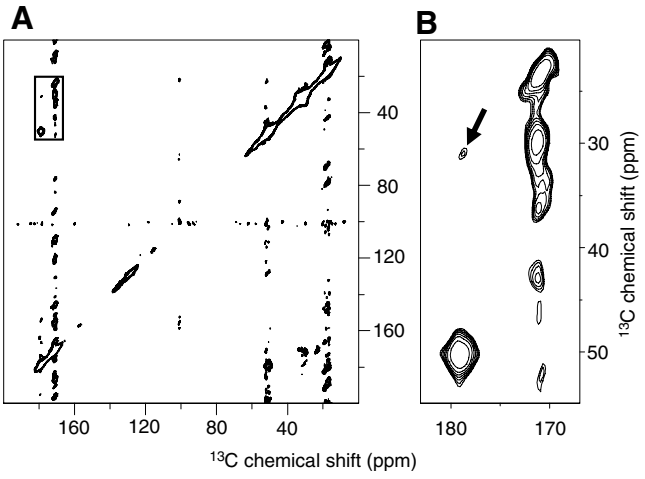

Figure 3. 2D R2 spectrum (mixing time = 50 ms, ns = 122,800, ns per t_1 point = 480) of Aβ42 aggregates uniformly labeled with ^{13}C and ^{15}N at Met-35 and Ala-42 (8.5 mg/tube). The MAS speed was 14,820 Hz, which corresponded to the difference between the chemical shifts of C_β and/or C_γ of Met-35 and C=O of Ala-42. (A) Whole spectrum. (B) Enlarged display of the spectrum framed by the bold line. The arrow shows a cross peak between C_β and/or C_γ of Met-35 and C=O of Ala-42.

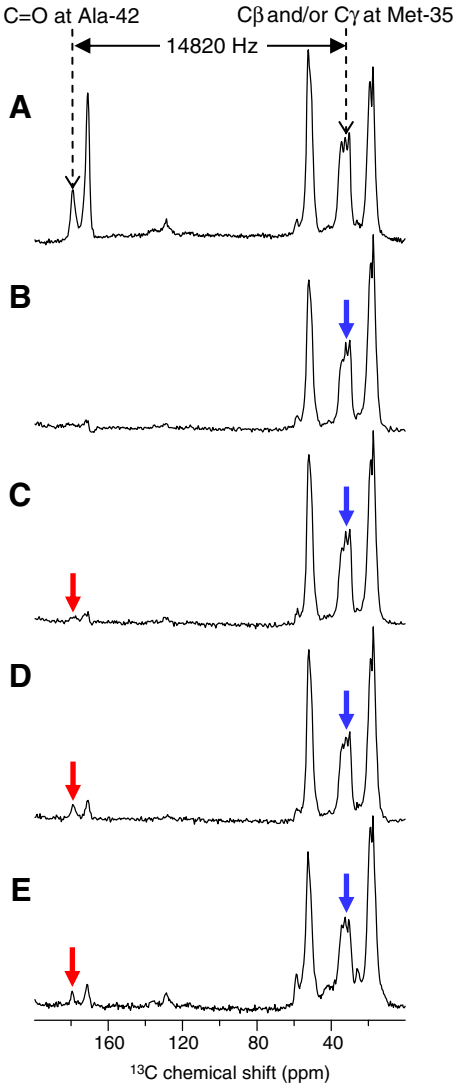

Figure 4. (A) 1D ^{13}C CP-MAS spectrum of Aβ42 aggregates uniformly labeled with ^{13}C and ^{15}N at Met-35 and Ala-42 (8.5 mg/tube). The MAS speed was 20,000 Hz. (B–D) 1D R2 spectrum of Aβ42 aggregates uniformly labeled with ^{13}C and ^{15}N. The mixing times were (B) 0.2 ms, (C) 16.7 ms, and (D) 50 ms (ns = 7,200). (E) 1D R2 spectrum of aggregates of labeled Aβ42 diluted with unlabeled Aβ42 at a ratio of 1:2 (14.0 mg/tube) at a mixing time of 50 ms (ns = 7,200). In the spectra of (B–E), the MAS speed was set to 14,820 Hz. Magnetization transfer from C_β and/or C_γ of Met-35 (blue arrow) to C=O of Ala-42 (red arrow) by the R2 effect was observed.

Our previous study on the systematic replacement of Aβ42 with proline revealed the existence of two β-strands at positions 35–37 and 40–42 separated by the turn at positions 38 and 39 (Fig. 1A).[6] Four structures are thus possible for the C-terminal β-sheets (Fig. 5). In the models of intermolecular β-sheets (Fig. 5A and B), bulky side chains (Val-40 or Ile-41) between the β-strands hinder the contact of Met-35 and Ala-42, resulting in a long distance between them (ca. 10 Å). On the other hand, the distance between C_β, C_γ of Met-35 and C=O of Ala-42 is about 4–6 Å

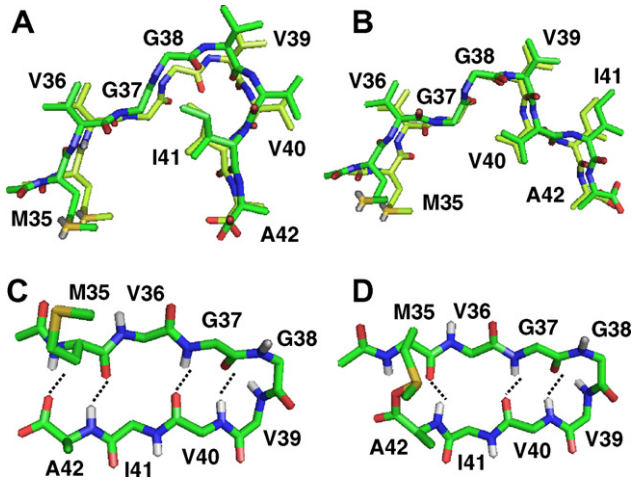

Figure 5. Possible structural models of the C-terminus of Aβ42 in aggregates: intermolecular β-sheets whose side chains of Val-39 and Val-40 are located on (A) the same or (B) the opposite side of the main chain, and intramolecular β-sheets (C) without or (D) with an S–O bond between the side chain of Met-35 and the carboxyl group of Ala-42. Dotted lines show hydrogen bonds. Modeling of the C-terminal structures was carried out using the biopolymer function in Sybyl 7.3 (Tripos, Inc.).

and 3–5 Å in the models of the intramolecular β-sheets without and with the S–O bond, respectively (Fig. 5C and D). Our present result using the R2 method suggests that at least some part of the intramolecular distance between C_β and/or C_γ of Met-35 and C=O of Ala-42 is shorter than 6 Å; this strongly supports the presence of the intramolecular antiparallel β-sheet structure (Fig. 5C and D). Although our result does not directly prove the presence of the S–O bond in Aβ42 aggregates, it is certain that the *S*-oxidized radical cation at Met-35 is able to interact with the C-terminal carboxylate anion to form the S–O bond.

This is the first report of proving the existence of a C-terminal intramolecular antiparallel β-sheet in Aβ42 aggregates. Formation of this β-sheet enables the association of the sulfur atom of Met-35 with the C-terminal carboxylate anion to stabilize the short-lived *S*-oxidized radical cation. The resultant hydrophobic core with no electrical charges (Fig. 1B) would accelerate the nucleation of Aβ42. Systematic proline replacement by Wetzel and colleagues proposed a model of Aβ40 aggregates without β-sheet in the C-terminus.[22] The mechanism verified in this study clearly explains the higher aggregative ability, neurotoxicity, and radical productivity of Aβ42 compared to Aβ40.

We observed at least two conformations or molecular species at Met-35 (Table 1); this implies that Aβ42 with the C-terminal intermolecular β-sheets (Fig. 5A and B) could also exist in the aggregates. Takano and coworkers have recently crystallized a fusion protein containing Aβ28–42's N-terminus and the C-terminal region of ribonuclease HII from a hyperthermophile, *Thermococcus kodakaraensis*, suggesting the existence of a similar intramolecular antiparallel β-sheet with a turn at positions 36 and 37 in the aqueous environment.[23] Although various structures might exist at the C-terminus of Aβ42 in the aggregates, a C-terminal core containing a radical (Fig. 5D) is most likely responsible for the aggregation and neurotoxicity of Aβ42. Structural analysis of each conformer is in progress in our laboratory.

Acknowledgments

This research was partly supported by grants-in-aid for Scientific Research (A) (No. 18208011 for K.I.) and the Promotion of Science for Young Scientists (No. 18.3327 for Y.M.) from the Ministry of Education, Science, Culture, Sports, and Technology of the Japanese Government. We thank Dr. H. Fukuda at the Institute of Medical Science, Tokyo University for measurements of MALDI-TOF-MS.

Supplementary data

Experimental section and supplementary figures are available via the internet. Supplementary data associated with this article can be found, in the online version, at doi:10.1016/j.bmcl.2008.04.060.

References and notes

1. Selkoe, D. J. *Nat. Cell. Biol.* **2004**, *6*, 1054.
2. Davis-Salinas, J.; Saporito-Irwin, S. M.; Cotman, C. W.; Van Nostrand, W. E. *J. Neurochem.* **1995**, *65*, 931.
3. Serpell, L. C. *Biochim. Biophys. Acta* **2000**, *1502*, 16.
4. Balbach, J. J.; Petkova, A. T.; Oyler, N. A.; Antzutkin, O. N.; Gordon, D. J.; Meredith, S. C.; Tycko, R. *Biophys. J.* **2002**, *83*, 1205.
5. Antzutkin, O. N.; Leapman, R. D.; Balbach, J. J.; Tycko, R. *Biochemistry* **2002**, *41*, 15436.
6. Morimoto, A.; Irie, K.; Murakami, K.; Masuda, Y.; Ohigashi, H.; Nagao, M.; Fukuda, H.; Shimizu, T.; Shirasawa, T. *J. Biol. Chem.* **2004**, *279*, 52781.
7. Varadarajan, S.; Yatin, S.; Aksenova, M.; Butterfield, D. A. *J. Struct. Biol.* **2000**, *130*, 184.
8. Barnham, K. J.; Masters, C. L.; Bush, A. I. *Nat. Rev. Drug Disc.* **2004**, *3*, 205.
9. Varadarajan, S.; Kanski, J.; Aksenova, M.; Lauderback, C.; Butterfield, D. A. *J. Am. Chem. Soc.* **2001**, *123*, 5625.
10. Schöneich, C. *Arch. Biochem. Biophys.* **2002**, *397*, 370.
11. Kanski, J.; Aksenova, M.; Schöneich, C.; Butterfield, D. A. *Free Radic. Biol. Med.* **2002**, *32*, 1205.
12. Murakami, K.; Irie, K.; Ohigashi, H.; Hara, H.; Nagao, M.; Shimizu, T.; Shirasawa, T. *J. Am. Chem. Soc.* **2005**, *127*, 15168.
13. Hexem, J. G.; Frey, M. H.; Opella, S. J. *J. Am. Chem. Soc.* **1981**, *103*, 224.
14. Naito, A.; Ganapathy, S.; McDowell, C. A. *J. Chem. Phys.* **1981**, *74*, 5393.
15. Takegoshi, K.; Nakamura, S.; Terao, T. *J. Chem. Phys.* **2003**, *118*, 2325.
16. Wishart, D. S.; Sykes, B. D. *J. Biomol. NMR* **1994**, *4*, 171.
17. Wishart, D. S.; Bigam, C. G.; Holm, A.; Hodges, R. S.; Sykes, B. D. *J. Biomol. NMR* **1995**, *5*, 67.
18. Raleigh, D. P.; Levitt, M. H.; Griffin, R. G. *Chem. Phys. Lett.* **1988**, *146*, 71.
19. Raleigh, D. P.; Creuzet, F.; Das Gupta, S. K.; Levitt, M. H.; Griffin, R. G. *J. Am. Chem. Soc.* **1989**, *111*, 4502.

20. Griffiths, J. M.; Griffin, R. G. *Anal. Chim. Acta* **1993**, *283*, 1081.
21. Lansbury, P. T., Jr.; Costa, P. R.; Griffiths, J. M.; Simon, E. J.; Auger, M.; Halverson, K. J.; Kocisko, D. A.; Hendsch, Z. S.; Ashburn, T. T.; Spencer, R. G. S.; Tidor, B.; Griffin, R. G. *Nat. Struct. Biol.* **1995**, *2*, 990.
22. Williams, A. D.; Portelius, E.; Kheterpal, I.; Guo, J. T.; Cook, K. D.; Xu, Y.; Wetzel, R. *J. Mol. Biol.* **2004**, *335*, 833.
23. Takano, K.; Endo, S.; Mukaiyama, A.; Chon, H.; Matsumura, H.; Koga, Y.; Kanaya, S. *FEBS J.* **2006**, *273*, 150.